

8-2017

# Angular Distribution of Single-Photon Superradiance in a Dilute and Cold Atomic Ensemble


A. S. Kuraptsev

I. M. Sokolov

M. D. Havey

Old Dominion University, mhavey@odu.edu

Follow this and additional works at: [https://digitalcommons.odu.edu/physics\\_fac\\_pubs](https://digitalcommons.odu.edu/physics_fac_pubs)

 Part of the [Atomic, Molecular and Optical Physics Commons](#), and the [Biological and Chemical Physics Commons](#)

---

## Repository Citation

Kuraptsev, A. S.; Sokolov, I. M.; and Havey, M. D., "Angular Distribution of Single-Photon Superradiance in a Dilute and Cold Atomic Ensemble" (2017). *Physics Faculty Publications*. 70.  
[https://digitalcommons.odu.edu/physics\\_fac\\_pubs/70](https://digitalcommons.odu.edu/physics_fac_pubs/70)

## Original Publication Citation

Kuraptsev, A. S., Sokolov, I. M., & Havey, M. D. (2017). Angular distribution of single-photon superradiance in a dilute and cold atomic ensemble. *Physical Review A*, 96(2), 023830. doi:10.1103/PhysRevA.96.023830

**Angular distribution of single-photon superradiance in a dilute and cold atomic ensemble**A. S. Kuraptsev,<sup>1</sup> I. M. Sokolov,<sup>1,2</sup> and M. D. Havey<sup>3</sup><sup>1</sup>*Department of Theoretical Physics, Peter the Great St. Petersburg Polytechnic University, 195251, St. Petersburg, Russia*<sup>2</sup>*Institute for Analytical Instrumentation, Russian Academy of Sciences, 198095, St. Petersburg, Russia*<sup>3</sup>*Department of Physics, Old Dominion University, Norfolk, Virginia 23529, USA*

(Received 26 January 2017; published 14 August 2017)

On the basis of a quantum microscopic approach we study the dynamics of the afterglow of a dilute Gaussian atomic ensemble excited by pulsed radiation. Taking into account the vector nature of the electromagnetic field we analyze in detail the angular and polarization distribution of single-photon superradiance of such an ensemble. The dependence of the angular distribution of superradiance on the length of the pulse and its carrier frequency as well as on the size and the shape of the atomic clouds is studied. We show that there is substantial dependence of the superradiant emission on the polarization and the direction of fluorescence. We observe essential peculiarities of superradiance in the region of the forward diffraction zone and in the area of the coherent backscattering cone. We demonstrate that there are directions for which the rate of fluorescence is several times more than the decay rate of the timed-Dicke state. We show also that single-photon superradiance can be excited by incoherent excitation when atomic polarization in the ensemble is absent. Besides a quantum microscopic approach, we analyze single-photon superradiance on the basis of the theory of incoherent multiple scattering in optically thick media (random walk theory). In the case of very short resonant and long nonresonant pulses we derive simple analytical expressions for the decay rate of single-photon superradiance for incoherent fluorescence in an arbitrary direction.

DOI: [10.1103/PhysRevA.96.023830](https://doi.org/10.1103/PhysRevA.96.023830)**I. INTRODUCTION**

Since the original work by Dicke [1], the problem of superradiance, and its counterpart subradiance, have attracted great interest. By the end of the 1980s many aspects of the physics of the superradiance problem had been studied in detail (see [2] and references therein). However, in the past decade, theoretical and experimental advances have led to a rejuvenation of this field. This rejuvenation connects with theoretical predictions [3,4] of the possibility to observe fast collective spontaneous decay in an atomic ensemble under conditions of very weak excitation. Such a type of fast decay along with the accompanying collective Lamb shift have been experimentally observed in the x-ray regime [5], in cold atoms [6–8], and in quantum dots [9]. It has become more or less conventional to designate these effects by the term “single-photon superradiance”.

Contrary to the “traditional” superradiance predicted by Dicke for polyatomic ensembles with sizes much smaller than the radiation wavelength, the single-photon superradiance is observed for large-sized systems. It differs also from well-studied superfluorescence of long and extended ensembles with a large number of initially excited atoms. Single-photon superradiance is a linear-optics effect and it can take place for dilute atomic systems under excitation by a weak pulse of radiation. By now the main features of these effects as well as closely related phenomena like optical precursors and the flash effect have been studied both theoretically and experimentally [5–14] (and references therein).

Due to the effect of coherent forward scattering, the main part of the radiation pulse absorbed by the extended atomic ensemble is scattered into directions close to that of the exciting light pulse [3,15]. In this connection the main attention was given to the properties of superradiance emitted in the forward direction. Particularly it was shown that one way to obtain strong coherent emission from the ensembles is to prepare

a timed-Dicke state [16]. However, as was shown in [17] and studied in a sophisticated experiment [7] superradiance can be observed in directions outside the bounds of the main diffraction cone. Moreover, the fluorescence decay rate in these directions can exceed the decay rate of the timed-Dicke state responsible for forward radiation. In several works [7,17] the time dependence of fluorescence in certain, fixed directions was studied. The main goal of the present paper is to study theoretically the angular distribution of superradiance in more detail. Among other things, we will show that superradiance is characterized by a strong and essentially nonmonotonic angular dependence.

In analysis of the angular dependence of single-photon superradiance, the polarization properties of the fluorescence may play an important role. In experiments [6,7] the total intensity of scattered light was measured. The polarization dependence was not analyzed in detail. For radiation coherently scattered into the forward direction the polarization of superradiance should coincide with that of incident light. In [6] it was experimentally confirmed in the case of the linear polarization of the excitation pulse. So the polarization need not be studied. In the case of sideways scattering it is not the case. Decay of fluorescence in different polarization channels has in the general case different rates. For this reason, in studying single-photon superradiance, we will make additional analysis of its polarization properties.

Another goal of the present work is to study the influence of the type of excitation on single-photon superradiance. For scattering in the main diffraction lobe this influence has been studied in great length. Particularly it has been discussed how the nature of superradiance changes if the initial state differs from a timed-Dicke state. In this work we will consider the influence of the pulse duration on the angular distribution of superradiance. Broadly speaking, single-photon excitation is not necessary for superradiance. In the paper [18] it was

shown that the initial spatially extended atomic coherence is important. In real optical experiments excitation of the atomic ensemble is performed by means of a light pulse. In experiment [6] it was a short pulse with a length less than the lifetime of the excited states of the free atom. In [7] the pulse duration exceeded essentially the lifetime. For a large detuning of the carrier frequency of the pulse the ensemble is optically thin and all atoms were excited with the same probability as in a timed-Dicke state. At the same time the scattering at a large angle is incoherent and this raises the question of whether coherent excitation is necessary for observation of single-photon superradiance beyond the main diffraction lobe. In this work we consider not only the dependence of the angular distribution of the superradiance on the length of the exciting pulse but also the possibility to observe superradiance in the case of noncoherent excitation. We will show that it is indeed possible.

Finally, we will study the dependence of the angular distribution of the decay rate on the shape of the atomic ensemble. We will consider how this distribution is modified by the change of the aspect ratio of an elliptical sample with a Gaussian density distribution.

## II. BASIC ASSUMPTIONS AND APPROACH

In our calculations of time-dependent fluorescence we will follow the theoretical approach developed previously in [19]. In the framework of this approach we solve the nonstationary Schrödinger equation for the wave function  $\psi$  of the joint system consisting of all atoms and a weak electromagnetic field. A vacuum reservoir is also included in our considerations.

We consider a disordered atomic cloud of  $N$  two-level atoms. All atoms have a ground state  $|g\rangle$  with the total angular momentum  $J_g = 0$ , an excited state  $|e\rangle$  with  $J_e = 1$ , a transition frequency  $\omega_a$ , and a natural lifetime of the excited state  $\tau_0 = 1/\gamma$ . Taking into account the experimentally relevant situation of a cold atomic cloud we assume atoms to be motionless and located at random positions  $\mathbf{r}_i$ , ( $i = 1, \dots, N$ ). Possible atomic displacement caused by residual atomic motion is taken into account by averaging of calculated quantities over random spatial distribution of the atoms.

We seek the wave function  $\psi$  as an expansion in a set of eigenfunctions of the Hamiltonian  $H_0$  of the noninteracting atoms and field. The key simplification of the approach employed is in the restriction of the total number of states taken into account. Assuming that the exciting radiation is weak, which is typical in experiments [6,7], we take into account only states with no more than one photon in the field. As it was shown in Refs. [20–24], this approximation allows us to describe collective effects under scattering of weak radiation, including pulsed radiation.

Knowledge of the wave function gives us information about the properties of the atomic ensemble as well as the properties of the secondary radiation. In particular, the intensity  $I_\alpha(\Omega, t)$  of the light polarization component  $\alpha$  that the atoms scatter in a unit solid angle around an arbitrary direction given by radius-vector  $\mathbf{r}$  ( $\Omega = \theta, \varphi$ ) can be determined as follows:

$$I_\alpha(\Omega, t) = \frac{c}{4\pi} \langle \psi | E_\alpha^{(-)}(\mathbf{r}) E_\alpha^{(+)}(\mathbf{r}) | \psi \rangle r^2. \quad (2.1)$$

Here  $E_\alpha^{(\pm)}(\mathbf{r})$  are the positive and negative frequency parts of the electric field operator.

In the case of pulsed excitation, the mean value in this expression depends on time. The corresponding dependence can be found as the inverse Fourier transform (for more details see [25]),

$$\langle \psi | E_\alpha^{(-)}(\mathbf{r}) E_\alpha^{(+)}(\mathbf{r}) | \psi \rangle = \left| \int_{-\infty}^{\infty} \frac{\hbar \exp(-i\omega t) d\omega}{2\pi} \times \sum_{e, e'} \tilde{\Sigma}_{\alpha e}(\omega) R_{ee'}(\omega) \Lambda_{e'}(\omega) \right|^2 \quad (2.2)$$

Here the vector  $\Lambda_e(\omega)$  describes excitation of different states of different atoms by external pulsed radiation,

$$\Lambda_e(\omega) = -\frac{\mathbf{d}_{e;g} \mathbf{E}(\omega)}{\hbar} = -\frac{\mathbf{u} \mathbf{d}_{e;g} E_0(\omega) \exp(i\mathbf{k}\mathbf{r}_e)}{\hbar}. \quad (2.3)$$

In this equation  $\mathbf{d}_{e;g}$  is the dipole matrix element for the transition from the ground  $g$  to the excited  $e$  state of the atom,  $E_0(\omega)$  is a Fourier amplitude of the probe radiation, which we assume to be a plane wave,  $\mathbf{k}$  and  $\mathbf{u}$  are its wave vector and unit polarization vector, and  $\mathbf{r}_e$  is the radius vector of the atom  $e$ .

The matrix  $R_{ee'}(\omega)$  is the resolvent of the considered system projected on the onefold atomic excited states,

$$R_{ee'}(\omega) = [(\omega - \omega_e)\delta_{ee'} - \Sigma_{ee'}(\omega)]^{-1}. \quad (2.4)$$

In this work we determine it numerically on the basis of the known expression for the matrix  $\Sigma_{ee'}(\omega)$ . Matrix elements  $\Sigma_{ee'}(\omega)$  for  $e$  and  $e'$  corresponding to different atoms describe excitation exchange between these atoms,

$$\Sigma_{ee'}(\omega) = \sum_{\mu, \nu} \frac{\mathbf{d}_{e_a;g_a}^\mu \mathbf{d}_{g_b;e_b}^\nu}{\hbar r^3} \times \left[ \delta_{\mu\nu} \left( 1 - i \frac{\omega_a r}{c} - \left( \frac{\omega_a r}{c} \right)^2 \right) \exp\left(i \frac{\omega_a r}{c}\right) - \frac{\mathbf{r}_\mu \mathbf{r}_\nu}{r^2} \left( 3 - 3i \frac{\omega_a r}{c} - \left( \frac{\omega_a r}{c} \right)^2 \right) \exp\left(i \frac{\omega_a r}{c}\right) \right]. \quad (2.5)$$

This expression is written assuming that in states  $\psi_{e'}$  and  $\psi_e$  atoms  $b$  and  $a$  are excited correspondingly, we used also the pole approximation ( $\Sigma_{ee'}(\omega) = \Sigma_{ee'}(\omega_a)$ ; see [26]). In (2.5)  $\mathbf{r}_\mu$  is projections of the vector  $\mathbf{r} = \mathbf{r}_a - \mathbf{r}_b$  on the axes of the chosen reference frame and  $r = |\mathbf{r}|$  is the spacing between atoms  $a$  and  $b$ .

If  $e$  and  $e'$  correspond to excited states of one atom then  $\Sigma_{ee'}(\omega)$  differs from zero only for  $e = e'$  (i.e.,  $m = m'$ , where  $m$  is magnetic quantum number of the atomic excited state). In this case,

$$\Sigma_{ee}(\omega) = -i\gamma/2. \quad (2.6)$$

The matrix  $\tilde{\Sigma}_{\alpha e}(\omega)$  in (2.2) describes light propagation from an atom excited in the state  $e$  to the photodetector. In the

rotating wave approximation it is (see [19])

$$\begin{aligned}\tilde{\Sigma}_{\alpha e}(\omega) &= -\frac{\mathbf{u}'_{\alpha}{}^* \mathbf{d}_{g:e}}{\hbar r} \left(\frac{\omega}{c}\right)^2 \exp\left(i\frac{\omega|\mathbf{r}-\mathbf{r}_e|}{c}\right) \\ &\approx -\frac{\mathbf{u}'_{\alpha}{}^* \mathbf{d}_{g:e}}{\hbar r} \left(\frac{\omega}{c}\right)^2 \exp\left(i\frac{\omega r}{c} - i\frac{\mathbf{k}'\mathbf{r}_e}{c}\right).\end{aligned}\quad (2.7)$$

Here  $\mathbf{u}'_{\alpha}$  is a unit polarization vector of the scattered wave and  $\mathbf{k}'$  is its wave vector.

Substituting (2.3) and (2.7) into (2.2), after some simplifications we have

$$\begin{aligned}I_{\alpha}(\Omega, t) &= \frac{c}{4\pi\hbar^2} \left| \int_{-\infty}^{\infty} E_0(\omega) k^2 \frac{\exp(-i\omega t) d\omega}{2\pi} \right. \\ &\quad \left. \times \sum_{e, e'} (\mathbf{u}'_{\alpha}{}^* \mathbf{d}_{g:e}) R_{ee'}(\omega) (\mathbf{u} \mathbf{d}_{e':g}) \exp(i(\mathbf{k}\mathbf{r}_{e'} - \mathbf{k}'\mathbf{r}_e)) \right|^2.\end{aligned}\quad (2.8)$$

The total intensity  $I(\Omega, t)$  can be obtained as a sum of (2.8) over two orthogonal polarizations  $\alpha$ .

Note that the coupled-dipole approach very similar to those described in this paper is used to analyze the atomic decay or dynamics of fluorescence in several works [26–40]. In the main part of the mentioned references, the scalar approximation was used. It is known that for the dilute clouds we are interested in here this approach is quite appropriate for a description of a whole series of properties [41–43] (if one takes into account that it underestimates optical thickness; see below). However, in the present work we are going to study the polarization dependence of fluorescence and we have to avoid this simplification.

In the next section, we will use relation (2.8) to analyze temporal, polarization, and angular properties of the scattered light.

### III. RESULTS AND DISCUSSION

In the present work we will consider axially symmetric Gaussian clouds having an average density distribution given by

$$n(\mathbf{r}) = n_0 \exp\left(-\frac{z^2}{2L^2} - \frac{x^2 + y^2}{2R^2}\right).\quad (3.1)$$

The incident light is a plane wave propagating in the  $z$  direction except for the case when we consider incoherent excitation. In the latter case we will consider quasi-isotropic irradiation from all directions. For illustrative purposes, we will restrict our consideration to temporally rectangular pulses having a central frequency  $\omega_L$ . The length of the pulse is  $\tau_L$ . We will assume that the zero-time reference  $t = 0$  corresponds to the end of the exciting pulse. In all calculations the incident light is left-handed circularly polarized.

In the following we will use Eq. (2.8) averaged over the ensemble of possible atomic configurations to study the average intensity of the time-dependent fluorescence  $\langle I_{\alpha}(\Omega, t) \rangle$ . Collective effects not only accelerate the fluorescence in some directions but also modify the functional form of  $\langle I_{\alpha}(\Omega, t) \rangle$  making it nonexponential. To analyze the peculiarities of the

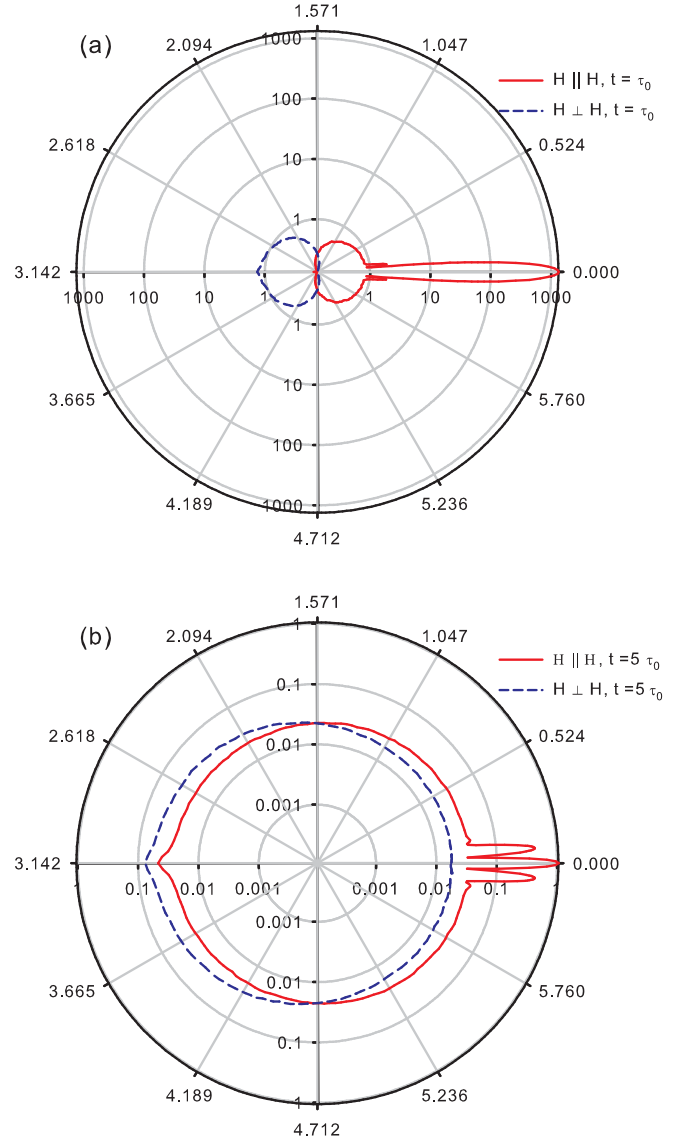


FIG. 1. Angular distribution of light scattered in different polarization channels for different times after the excitation pulse is switched off. (a)  $t = \tau_0$ ; (b)  $t = 5\tau_0$ . Spherically symmetric Gaussian cloud  $L = R = 25\lambda$ ,  $n_0\lambda^3 = 0.005$ . Pulse length is  $\tau_L = 0.1\tau_0$ .

time dependence we introduce a current decay rate as follows:

$$\Gamma_{\alpha}(\Omega, t) = -\frac{\partial \ln \langle I_{\alpha}(\Omega, t) \rangle}{\partial t}.\quad (3.2)$$

For the total fluorescence without polarization analysis we will use a similar relation but with summed intensity  $\langle I(\Omega, t) \rangle = \sum_{\alpha} \langle I_{\alpha}(\Omega, t) \rangle$ .

#### A. Angular distribution of scattered light

In Fig. 1 we show the angular distribution of light scattered in different polarization channels. The calculation is performed for a spherically symmetric atomic ensemble. The radius of the Gaussian distribution is  $R = L = 25\lambda$ . Hereafter in this paper we use  $\lambda$  as a unit of length, where  $\lambda = \lambda/2\pi$ . The peak density is  $n_0 = 0.005$ . Figure 1(a) corresponds to a time equal to  $t = \tau_0$  after the exciting pulse is switched off. It demonstrates very

different behaviors for different polarizations of the scattered light. In the helicity preserving channel ( $H\parallel H$ ) we see a typical diffraction picture. There is a large main diffraction peak. Two higher order peaks are also well distinguished. The scattering into the back half-sphere is suppressed in this polarization channel. For the helicity-nonpreserving ( $H\perp H$ ) polarization channel the main part of the radiation is scattered into the backward direction. The intensity is mainly determined by single scattering from the boundary region. For the  $H\parallel H$  channel single scattering in the exact backward direction is absent because of selection rules for atomic electric dipole transitions.

The angular distribution of fluorescence changes with time. In Fig. 1(b) this effect is shown for  $t = 5\tau_0$ . For this time, the main contribution to the fluorescence is determined by multiply scattered light. The difference between polarization channels becomes less evident. Further, the angular distribution becomes more spherically symmetric in each channel. However, even at this time interval we see some traces of a diffraction picture. In both channels we see also the cone-shaped feature associated with coherent backscattering (see, for example, reviews [44,45] and references therein). The enhancement factor for the helicity preserving channel is close to two which is typical for a 0-1 transition. For another channel it is much less because of the single scattering contribution to the background [44,45].

We calculated angular dependencies like those shown in Fig. 1 for different instants of time and thus determined the current decay rate (3.2) for fluorescence in any direction and for any polarization channels. Consider at first, however, the decay rate for the total intensity as it was made in experiments [6,7].

In Fig. 2 we show the angular dependence of  $\Gamma(\Omega, t)$  averaged over some time intervals  $\Delta t$ . For a clearer demonstration we displaced the graphs along the abscissa.

Figure 2 demonstrates the essential angular dependence, especially near the forward and backward directions. Such dependence takes place for all considered time intervals. For the short time after the excitation pulse is switched off the superradiance is observed for radiation emitted in any directions (solid line). For the very beginning of the fluorescence the sideways scattering is characterized by a faster decay than a forward one.

The maximal decay rate corresponds to an angle which depends on the size of the system (see below). Beginning with some time, the decay rate changes the sign for definite angular intervals. This means that for corresponding time and angular intervals the intensity of fluorescence increases. Here we see the manifestation of oscillation in the afterglow of the atomic ensemble connected with quantum beating and caused by interference of light scattering through different collective states (see [5,6,17]).

In Fig. 2(b) we show the angular dependence of the decay rate for the region of the diffraction pattern on a large scale. One can see that the diffraction picture transforms with time. Particularly, the separation between pairs of diffraction peaks changes. In our view, the transformation of the diffraction pattern is responsible for the unusual angular dependence shown in Fig. 2. The intensity in a given direction changes not only because of decay of collective states but also because

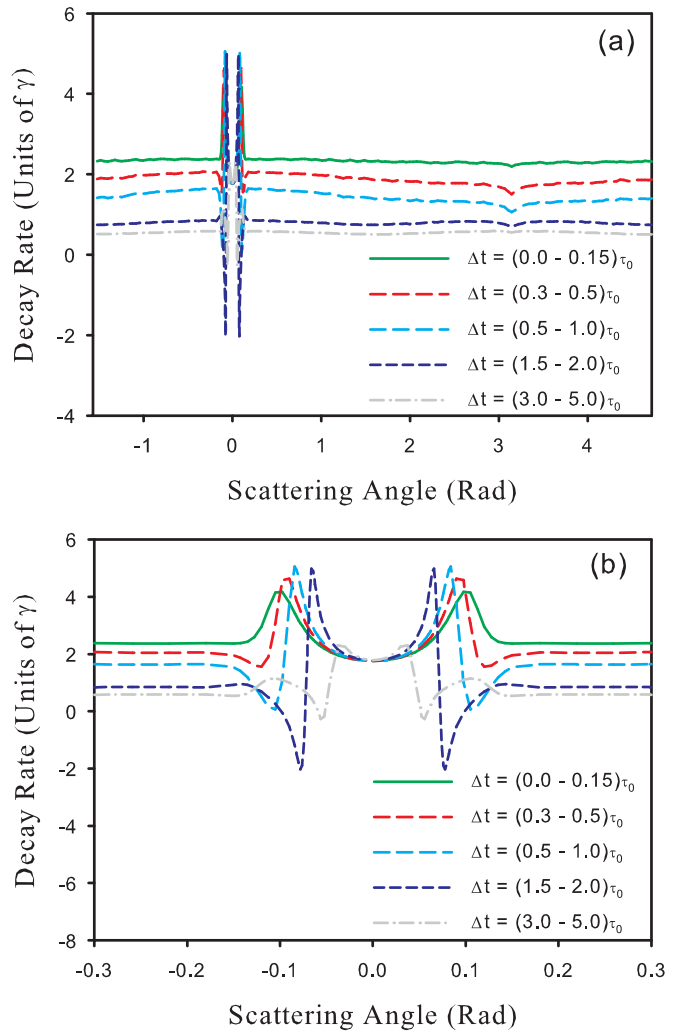


FIG. 2. Angular distribution of averaged decay rate  $\Gamma(\Omega, t)$  for different time intervals  $\Delta t$ . (a) Full range of scattering angles; (b) diffraction region. Calculations have been performed for the same parameters as Fig. 1.

of alteration in the direction of emission. The maximal decay rate is observed in directions of diffraction minima.

The difference in decay rates (3.2) for different directions of fluorescence is shown also in Fig. 3. Just after the end of the exciting pulse ( $t = 0$ )  $\Gamma(\Omega, 0) > \gamma$  for any direction. As time passes  $\Gamma(\Omega, t)$  changes. The afterglow into the forward direction maintains a high value for the longest period of time. For  $t$  up to  $t = 4\tau_0$  its value practically coincides with  $\Gamma(0, 0)$ . It means that for this period of time the contribution of the timed-Dicke state into the forward emission is dominant. The decay rate of radiation into the backward half-sphere ( $\theta > \pi/2$ ) decreases monotonically and for the considered condition it loses its superradiant properties for  $t \geq \tau_0$ . Fluorescence into diffraction minima and higher order maxima demonstrate nonmonotonic, oscillatory behavior. Two curves for  $\theta = 0.065$  and  $\theta = 0.075$  show that the decay rate can increase several times during the afterglow as well as decrease up to relatively large negative values.



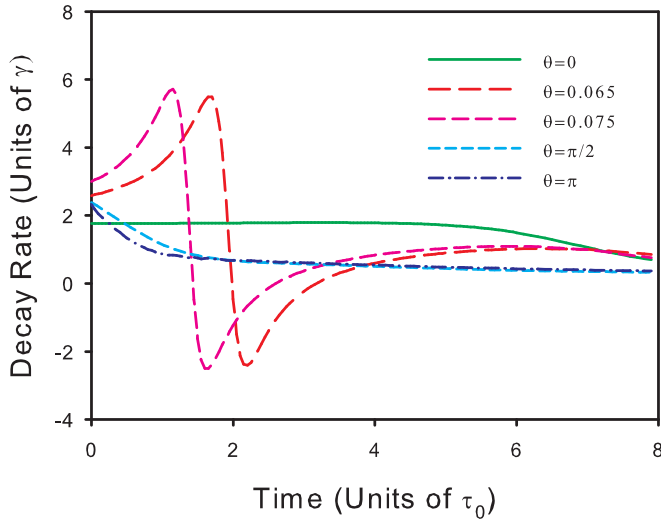


FIG. 3. Time dependence of the current decay rate of the fluorescence in different directions. Calculations have been performed for the same parameters as Figs. 1 and 2.

The dynamics of the fluorescence in different polarization channels (see Fig. 4) is even more complicated than that of the total light intensity. It is connected with the absence of single scattering in these channels into some specific direction. That is why the light intensity increases just after the pulse ends in the forward direction for the case of  $H \perp H$  and for the backward direction for  $H \parallel H$ . In these directions the decay rate (3.2) is negative and is relatively large in absolute value. With time the contribution of high order scattering increases and we observe the usual decreasing of decay rate.

**B. Dependence on type of excitation**

**1. Dependence on the excitation duration**

In many cases, in theoretical papers devoted to single-photon superradiance the decay of the timed-Dicke state is discussed. However, excitation of a real physical system into such a state is a separate and difficult problem. The authors of [5] found an original way to do so. In more traditional experiments with cold gases the excitation is performed by means of pulsed radiation. The length of the pulse strongly influences the type of prepared atomic states and the consequent fluorescence. In the case of a short pulse many different collective states in a wide spectral region are excited and the type of decay may differ essentially from the decay of a timed-Dicke state. In the case of a very long pulse we have a quasi-steady-state distribution of atomic excitation which differs from the distribution of the Dicke state. For the resonant excitation it is connected with absorption and for a nonresonant one with dispersion [21,22]. The spatial distribution of phases of the atomic oscillators is determined not by the wave number of the exciting light but by the light wavelength in the medium.

The dependence of the nature of decay on the type of excitation for the forward scattering was discussed earlier (see, for example, [5,18,46,47]). We will focus our attention on its influence on the angular distribution of single-photon

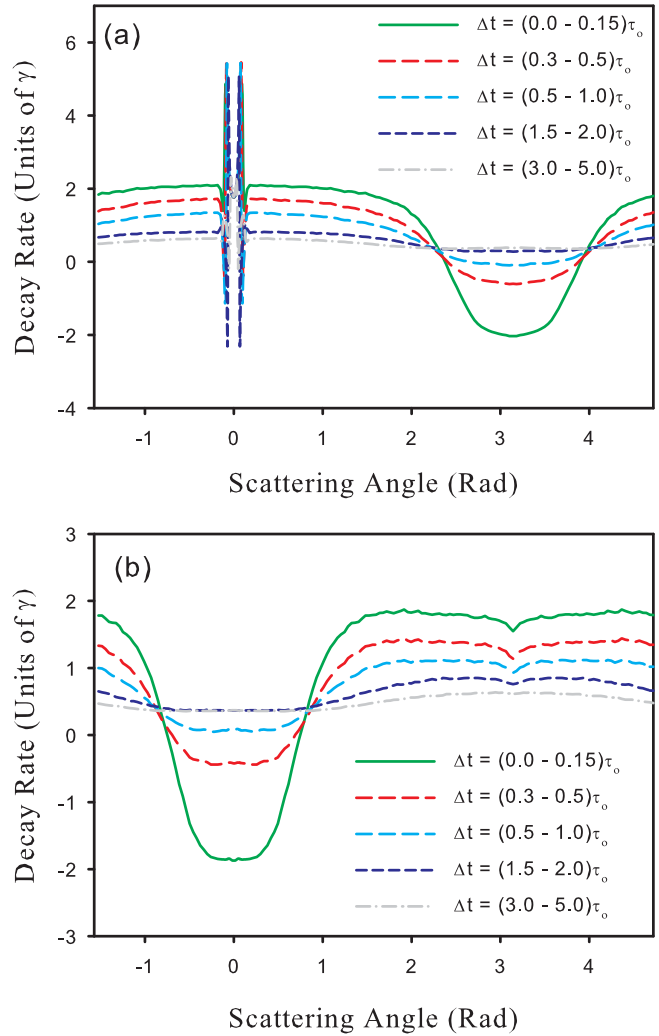


FIG. 4. Angular distribution of averaged decay rate  $\Gamma_\alpha(\Omega, t)$  for different polarization channels. (a)  $H \parallel H$ ; (b)  $H \perp H$ .  $\tau_L = \tau_0$ . The other parameters are as in Fig. 1.

superradiance. The corresponding dependence for the most interesting angular region is shown in Fig. 5. We demonstrate the angular dependence of decay rate both for very short and very long pulses. For the exact forward direction we see the weakest changes when the length of the pulse changes. It is connected with the fact that short-lived collective states responsible for forward scattering have a larger width and they are effectively excited independently of pulse length (spectral width of the pulse).

For the directions where we observe a sharp angular dependence the length of the pulse influences at the very beginning of fluorescence. Because of the spatial inhomogeneity of Gaussian clouds the length of the resonant pulse causes transformation of not only longitudinal (along light propagation) but also the transverse distribution of excited atoms. In its turn it causes transformation of the diffraction patterns.

Besides changes in width of the diffraction pattern we see a qualitative difference in angular dependence. For  $\tau_L = 0.1 \tau_0$  there is only relatively small maxima whereas already for

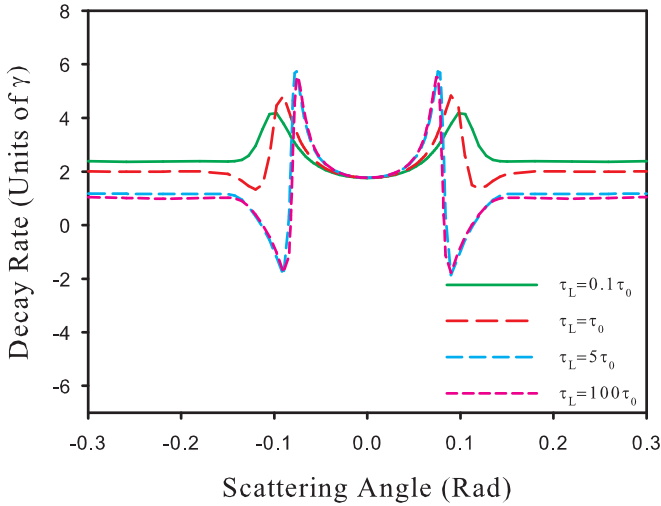


FIG. 5. Angular distribution of the decay rate for fluorescence excited by pulses of different length. Calculations have been performed for the same parameters as Fig. 1. Observation time interval is  $\Delta t = (0 - 0.1)\tau_0$ .

$\tau_L = 5\tau_0$  the maxima become more sharp, their amplitudes decrease essentially with angles, and in some regions the decay rate changes sign. For further increasing of  $\tau_L$  we observe only small quantitative changes. A saturation-type effect takes place. Increasing  $\tau_L$  from  $\tau_L = 5\tau_0$  up to  $\tau_L = 100\tau_0$  practically changes neither intensity of fluorescence nor its rate. It means that for the considered cloud for  $t = 5\tau_0$  quasi-static regime is realized.

The influence of excitation duration on fluorescence is also demonstrated in Fig. 6. Here we show the time dependence of the decay rate of fluorescence in different directions for two pulse lengths  $\tau_L = 0.1\tau_0$  and  $\tau_L = 100\tau_0$ . The qualitative difference between short (a) and long (b) excitation is that for a long pulse there are directions for which intensity begins to increase immediately after the end of the pulse. Figure 6 shows also that the excitation duration changes the nature of quantum beating.

## 2. Single-photon superradiance for incoherent excitation

The features of decay of a timed-Dicke state are essentially connected with phase matching of different atomic oscillators in the ensemble. Superradiance beyond the diffraction zone is caused by incoherent scattering. In this connection the question arises whether it is necessary to use coherent excitation to observe sideward superradiance. Or it is possible to observe this superradiance for incoherent excitation for complete absence of phase correlation. We performed calculation of atomic fluorescence assuming that different atoms in the Gaussian cloud are excited independently. In such a case the phases of different atoms are random and average atomic polarization is absent.

Analyzing the time dependence of the fluorescence we calculated the current decay rate for an exciting pulse of different lengths. The results are shown in Fig. 7.

The calculation was made for the case when the carrier frequency of the pulse coincides with the resonant frequency of the free atoms. It is seen that for short pulses we observe

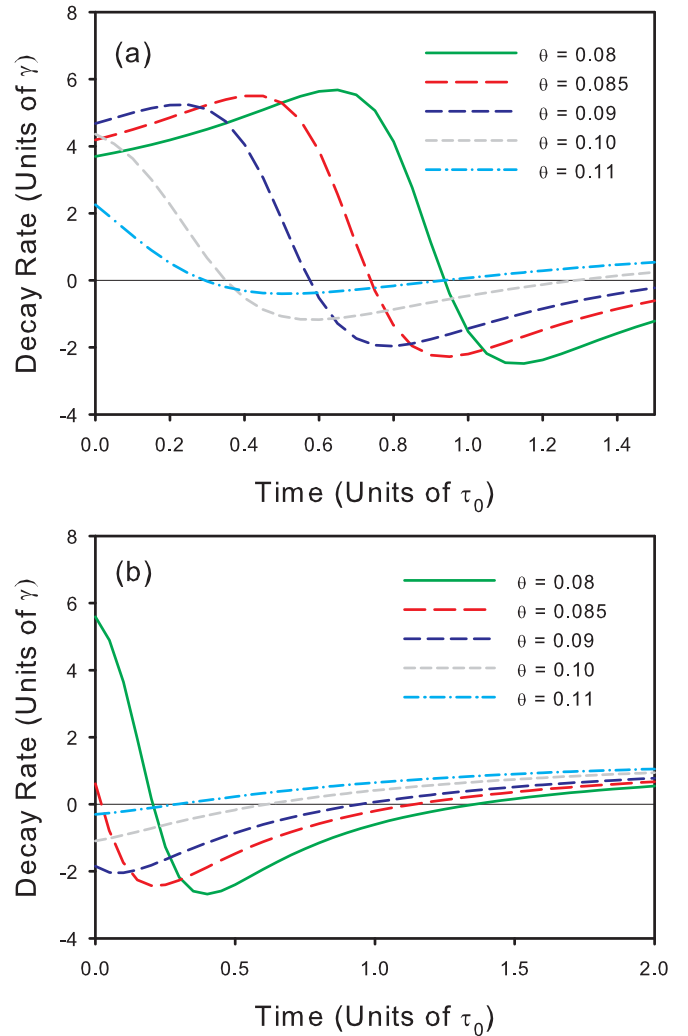


FIG. 6. Time dependence of the decay rate of fluorescence in different directions  $\theta$ . (a)  $\tau_L = 0.1\tau_0$ ; (b)  $\tau_L = 100\tau_0$ . The other parameters are as in Fig. 1.

a decay with a rate that exceeds the decay rate of the free atom, i.e., we observe superradiance. For long resonant pulses the superradiance is absent. However, in the paper [7] it was shown that long coherent nonresonant excitation causes superradiance of fluorescence in sideways directions. For this reason we studied how the decay rate depends on carrier frequency of the radiation in the case of incoherent excitation.

In Fig. 8 we show the corresponding dependence for two lengths of the pulse. The calculation is made for a spherically symmetric Gaussian cloud with radius  $R = 25$  and peak density  $n = 0.005$ . Because of spherical symmetry (on average) of the cloud and excitation the secondary radiation of the atomic ensemble is spherically symmetric.

For the short pulse  $\tau_L = 0.1\tau_0$ , and because of its large spectral width the decay rate does not practically depend on carrier frequency. On the contrary for long pulse  $\tau_L = 100\tau_0$  we see an essential dependence and, like in the case of coherent excitation [7], increasing of detuning causes increasing of decay rate up to some constant magnitude which depends on the size of the cloud, density, and which exceeds  $\gamma$ . The typical region of essential alteration of the rate is about the natural

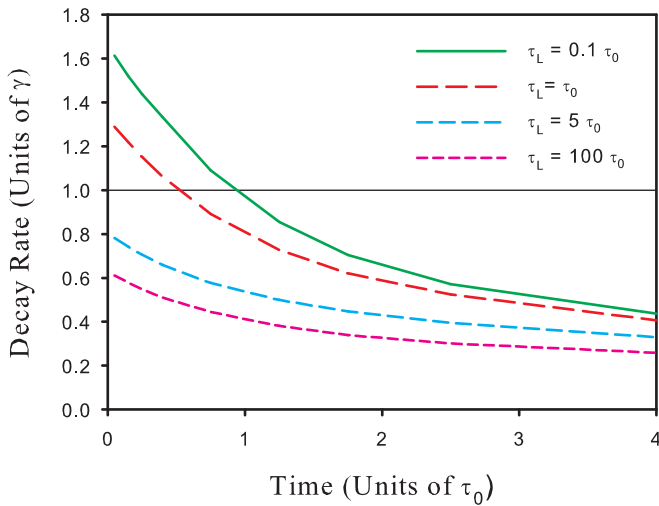


FIG. 7. Time dependence of the decay rate of fluorescence in the case of incoherent excitation by radiation of different pulse lengths. The other parameters are as in Fig. 1.

width of the transition of the free atom. For this spectral region the optical depth of the cloud is big and for long pulses we have a quasi-steady-state regime of atomic excitation. The atomic excitation under such conditions is determined not only by the external radiation but also by trapped light [22]. By the time of the end of the exciting pulse, the fluorescence is determined by photons scattered a different number of times inside the medium. For optically dense media scattering of high order plays an important role. After the end of the pulse we still see contributions of different order scattering but only the single scattering is responsible for superradiance. The contributions of higher order decay are much slower. That is why we do not see superradiance for long resonant pulse excitation. For nonresonant light the optical thickness is small and single scattering in the sideways direction gives the main contribution and superradiance can be seen.

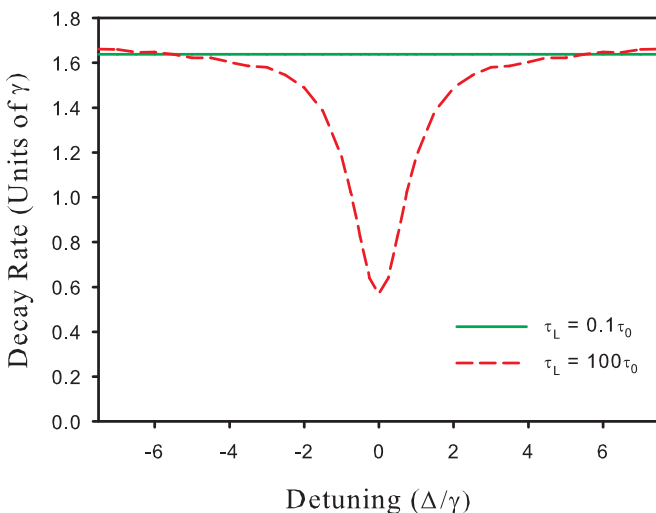


FIG. 8. Spectral dependence of the decay rate of fluorescence excited by incoherent radiation of different pulse durations. The decay rate is calculated for the time interval  $\Delta t = (0 - 0.1)\tau_0$  after the end of the exciting pulse. The other parameters are as in Fig. 1.

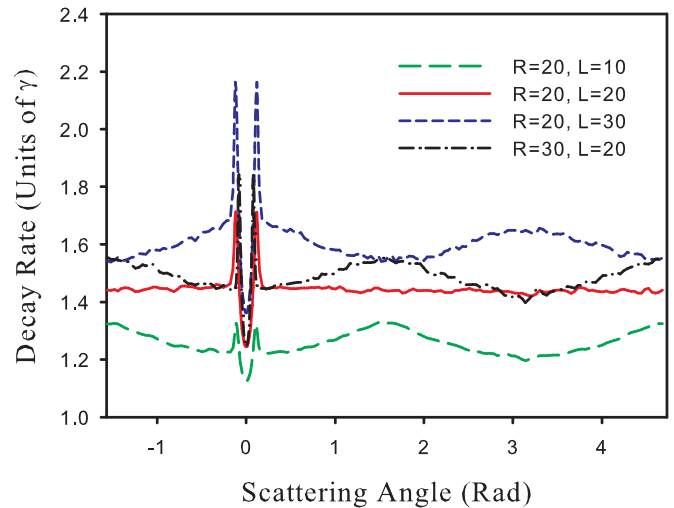


FIG. 9. Angular dependence of the decay rate of fluorescence excited by pulsed radiation of different durations. Decay rate is calculated for the time interval  $\Delta t = (0 - 0.1)\tau_0$  after the end of the exciting pulse.  $n_0 = 0.002$ . Pulse length is  $\tau_L = 0.1\tau_0$ .

### C. Single-photon superradiance for ensembles of different sizes

In this section we consider the dependence of angular distribution of superradiance on the sizes of the atomic ensemble. We will analyze both dependence on longitudinal and transverse sizes.

Let us consider at first how the angular distribution of the decay rate changes with length  $L$  of the Gaussian clouds for fixed transverse radius  $R$ . Results of the corresponding calculations for several  $L$  and  $R = 20$  are shown in Fig. 9. The density in the center of the atomic ensemble is equal to  $n = 0.002$ . The decay rate increases with  $L$  for all directions. But the specific dependence is different for different angles  $\theta$ .

For the forward direction we have

$$\Gamma(\theta = 0, t \rightarrow 0) = \gamma \left( 1 + \frac{b_{0z}}{8} \right), \quad (3.3)$$

where  $b_{0z} = \sqrt{2\pi}\sigma_0 n_0 L$  is the maximal resonant thickness of the Gaussian cloud along the  $z$  direction. This expression coincides with results obtained earlier in [47] if we take into account that the authors of [47] considered a scalar depth model of the radiation which underestimates the optical depth of the cloud by the factor 1.5.

The scattering in the near backward direction requires special attention. We see that for oblong clouds the decay rate into this direction ( $\theta = \pi$ ) even exceeds that for a timed-Dicke one ( $\theta = 0$ ). Note also that the decay rate for fluorescence at  $\theta = \pi/2$  also increases in spite of the fact that the transverse size is fixed.

Such angular dependence as well as many important regularities of single-photon superradiance can be understood in the framework of a random walk approach without analysis of collective states of a polyatomic ensemble usually used in such a case. The random walk approach is very effective for description of incoherent multiple scattering in optically thick but dilute media (see, for example, [48–51]). The light transport in a dilute medium generally performs a



diffusion-type process, which in a semiclassical picture can be visualized as a zigzag-type path consisting of segments of forwardly propagating waves. The forwardly propagating incoming, secondary, and multiply scattered waves can be expressed via a retarded-type Green's propagation function. The incoherent scattering events, which randomly happen in the medium, can be probabilistically simulated and properly described with the scattering theory formalism.

In practically important cases when sideward superradiance is observed, i.e., for short resonant or long nonresonant pulses the time dependence of the incoherent fluorescence, just after the end of the exciting pulse, can be described by taking into account only single incoherent scattering. The single scattering approximation is valid for a not very big average optical depth  $\bar{b}_0$  of the cloud  $-\bar{b}_0\tau_0/\tau_L \lesssim 1$  (for short pulses) or  $\bar{b}_0\tau_0\Delta_L \lesssim 1$  (for long nonresonant pulse). In such cases the intensity  $I_\alpha^s(\Omega, t)$  can be calculated as follows:

$$I_\alpha^s(\Omega, t) = \int \frac{cn(\mathbf{r}_a)}{4\pi\hbar^2} d^3r_a \left| \int_{-\infty}^{\infty} E_0(\omega) \frac{\exp(-i\omega t) d\omega}{2\pi} \times k^2 \chi(\mathbf{r}, \mathbf{r}_a, \omega) \sum_e \frac{(\mathbf{u}^* \mathbf{d}_{g:e})(\mathbf{u} \mathbf{d}_{e:g})}{\omega - \omega_a + i\gamma/2} \chi(\mathbf{r}_a, \mathbf{r}_0, \omega) \right|^2. \quad (3.4)$$

Here the function  $\chi(\mathbf{r}_a, \mathbf{r}_0, \omega)$  describes propagation of light from the source to the point  $\mathbf{r}_a$  where a single incoherent scattering event takes place. The function  $\chi(\mathbf{r}, \mathbf{r}_a, \omega)$  describes propagation of a secondary photon toward the photodetector. In the isotropic medium these functions are determined as follows:

$$\chi(\mathbf{r}_2, \mathbf{r}_1, \omega) = \exp\left(-\frac{ib_0(\mathbf{r}_2, \mathbf{r}_1)}{2} \frac{\gamma/2}{\omega - \omega_a + i\gamma/2}\right), \quad (3.5)$$

where the resonant optical thickness of the inhomogeneous cloud between points  $\mathbf{r}_1$  and  $\mathbf{r}_2$  for the considered case of the  $J = 0 \leftrightarrow J = 1$  transition is

$$b_0(\mathbf{r}_2, \mathbf{r}_1) = 6\pi\lambda^2 \int_{\mathbf{r}_1}^{\mathbf{r}_2} n(\mathbf{r}) ds. \quad (3.6)$$

Expression (3.4) can be used for calculation of the decay rate for all directions except in the zones of backward and forward scattering. For forward scattering the main contribution comes from the coherent component of the scattering light and for the backward direction one of the polarization components is absent for single scattering and scattering of higher order should be taken into account. Equation (3.4) is also not valid for the cloud with a large aspect ratio. In such a case diffraction effects play an essential role [52,53] and the propagation function  $\chi$  cannot be described by Eq. (3.5).

The integral over frequency  $\omega$  in (3.4) can be calculated on the basis of the theory of residues. Restricting by the case of a typical experimental situation without polarization analysis and taking into account that for rectangular pulse for  $t > \tau_L$

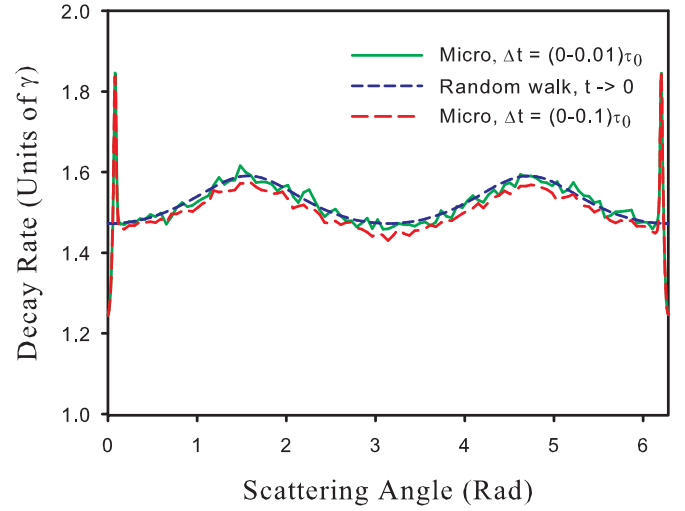


FIG. 10. Angular dependence of the decay rate of fluorescence. Comparison with analytical expression (3.7);  $\tau = 0.01\tau_0$ ,  $L = 20$ ,  $R = 30$ . The curves obtained in the microscopic approach were calculated as a result of averaging over approximately 20 000 different random spatial configurations of the atomic ensemble and were not smoothed. The fluctuations in the curves demonstrate the accuracy of the calculations.

only the pole  $\omega = \omega_a - i\gamma/2$  is important, we have

$$\begin{aligned} \Gamma(\Omega, t \rightarrow 0) &= \gamma \left(1 + \frac{\bar{b}_0(\mathbf{r})}{2}\right) \\ &= \gamma \left(1 + \frac{b_{0z}}{8} \left(1 + \frac{\sqrt{2}R}{\sqrt{R^2 + L^2 + (R^2 - L^2)\cos(2\theta)}}\right)\right). \end{aligned} \quad (3.7)$$

Here  $b_0(\mathbf{r})$  is the total optical length of the resonant light ray coming from the source and incoherently scattered in the point  $\mathbf{r}$  toward the detector located along the direction  $\theta$ ;  $\bar{b}_0(\mathbf{r})$  is the value averaged over all atoms in the cloud.

In Fig. 10 we demonstrate the adaptability of Eq. (3.7) for a description of the angular distribution of the decay rate of single-photon superradiance. In this figure we compare results of a quantum microscopic approach and approximate calculation of  $\Gamma(\Omega, t \rightarrow 0)$  on the basis of Eq. (3.7). It is clear that for a very small time interval  $\Delta t = (0 - 0.01)\tau_0$  we have a good qualitative agreement. For bigger intervals  $\Delta t = (0 - 0.1)\tau_0$  some quantitative discrepancy caused by scattering of higher order appears, but qualitatively the angular dependence of  $\Gamma(\Omega, t \rightarrow 0)$  is reproduced by Eq. (3.7) quite well.

Note that in much the same way as we get Eq. (3.7), we can obtain expression (3.3) for forward scattering if we consider only the coherent component of transmitted light.

Good agreement between a microscopic approach and a single scattering random walk approximation allows us to give a simple explanation of sideward superradiance in the considered cases. The calculation based on Eq. (3.4) shows that independently of the carrier frequency of the pulse the properties of secondary radiation after single scattering are

determined by optical depth of the cloud for quasiresonant radiation. Physically it is connected with the known fact that without external action any vibrating system oscillates at its eigenfrequencies. For dilute media these frequencies are close to the free atom resonant frequency. Propagation of such quasiresonant radiation in the considered dispersive medium is accompanied by substantial spectral transformation. For not very big optical depth this propagation leads to broadening of the spectrum and consequently to acceleration of fluorescence. For large optical depth distortion of the spectrum can be more essential. In such a case scattering of higher orders should be taken into consideration.

Finally, we make the important point that Eq. (3.4) also implies that, within this model, the superradiant signals in the sideways direction, for an unpolarized ground-state medium, should approximately have the same optical polarization as that of light scattered from a single atom. This means that for the optical transition case considered here, linearly polarized excitation would imply a 100% linear polarization degree of the scattered light. However, for different transitions  $F - F'$  the result will be different. For superradiance on an  $F = 2 \rightarrow F' = 3$  transition as studied recently in the sideways direction [7], the linear polarization degree would be about 9/28 in the traditional  $90^\circ$  geometry. This result would serve as a nice test of this interpretation of the sideways superradiance.

#### IV. CONCLUSIONS

In this paper we analyzed the time-dependent fluorescence of dilute Gaussian clouds of cold atoms excited by a weak quasi-resonant light pulse. The calculation was performed on the basis of the quantum microscopic approach. Solving the nonstationary Schrödinger equation for the joint system consisting of atoms and a weak electromagnetic field we calculated the angular distribution and polarization properties of the fluorescence.

We focused our attention on the initial stage of fluorescence where superradiance was expected. Calculating transformation of the angular distribution of the afterglow of the ensemble with time we observed that for total emission without polarization analysis superradiance took place in any direction if the length of the pulse less or comparable with natural lifetime of atomic excited states. Besides that there is substantial dependence of superradiance on the direction of fluorescence, especially in the region of the diffraction pattern and in the angular area of the coherent backscattering cone. Maximal decay rate is observed not for the forward direction but at some angle which is determined by the transverse size of the cloud. This maximal value is several times more than the decay rate of the timed-Dicke state. Time-dependent fluorescence in separate polarization channels is more complicated. For a short exciting pulse there are directions where the corresponding polarization component does not decrease, but increases initially. For example, for the helicity preserving channel it takes place for a direction close to the backward direction, for nonpreserving channels we see increasing of intensity into the forward direction.

For long coherent pulses the nature of fluorescence decay essentially depends on the frequency as was predicted in [7]. For resonant radiation the superradiance is observed only in the forward direction. Moreover, there are directions near the

main diffraction maximum where the total intensity summed over two orthogonal polarizations increases just after the end of exciting pulse. As the carrier frequency shifts from exact atomic resonance the decay rate in sideward directions increases and for some detunings superradiance takes place (see also [7]).

We repeated analysis of single-photon superradiance for the incoherent excitation and found that the superradiance can be observed in this case, i.e., when atomic polarization in the ensemble is absent. It can be excited either by a short pulse or by a long nonresonant one.

We studied the dependence of the angular distribution of superradiance on the size and shape of the atomic ensemble. Besides a sharp feature connected with the diffraction pattern, and the coherent backscattering cone, we observed noticeable transformation of this dependence caused by changes in the aspect ratio of the cloud. The decay rate is determined by average optical depth of the cloud for singly scattered photon.

Besides a quantum microscopic approach we analyzed single-photon superradiance on the basis of random walk theory. We showed that for not very big optical depth of the cloud, and in the case of very short resonant and long nonresonant pulses, the time dependence of the incoherent fluorescence just after the end of the pulse can be described by taking into account only single incoherent scattering. In such a case we derive simple analytical expressions for the decay rate of single-photon superradiance in an arbitrary direction.

The random walk approach has some advantages compared to exact coupled-dipole computations applied in the first part of our work. It gives us the opportunity to interpret the observed effects as a result of the light spectral shape transformation in dispersive media. Besides that it can be used for dilute atomic ensembles consisting of a macroscopic number of atoms, for example, prepared in a magneto-optical or optical dipole trap. In the framework of this approach we can take into account hyperfine structure of excited and ground states of the atoms, atomic motion, possible nonuniform population of different Zeeman sublevels of the ground states, i.e., possible orientation of atomic angular momentum. Scattering of any order also can be taken into account. In our opinion this approach can be also applied in the presence of a control field. Such a field changes the spectral properties of the medium essentially which strongly influences the incoherent scattering under conditions of electromagnetically induced transparency [54,55] and may modify single-photon superradiance in cold and dilute atomic gases.

#### ACKNOWLEDGMENTS

We appreciate financial support from the Russian Foundation for Basic Research (Grant No. RFBR-15-02-01013). A.S.K. acknowledges Grant No. RFBR-16-32-00587 and the Council for Grants of the President of the Russian Federation. We also acknowledge financial support from the National Science Foundation (Grant No. NSF-PHY-1606743). The results of the work were obtained using computational resources of Peter the Great Saint-Petersburg Polytechnic University Supercomputing Center (<http://www.spbstu.ru>).

- [1] R. H. Dicke, *Phys. Rev.* **93**, 99 (1954).
- [2] M. Gross and S. Haroche, *Phys. Rep.* **93**, 301 (1982).
- [3] M. O. Scully, E. S. Fry, C. H. R. Ooi, and K. Wódkiewicz, *Phys. Rev. Lett.* **96**, 010501 (2006).
- [4] M. O. Scully, *Laser Physics* **17**, 635 (2007).
- [5] R. Röhlsberger, K. Schlage, B. Sahoo, S. Couet, and R. Ruffer, *Science* **328**, 1248 (2010).
- [6] S. J. Roof, K. J. Kemp, M. D. Havey, and I. M. Sokolov, *Phys. Rev. Lett.* **117**, 073003 (2016).
- [7] M. O. Araujo, I. Kresic, R. Kaiser, and W. Guerin, *Phys. Rev. Lett.* **117**, 073002 (2016).
- [8] R. A. de Oliveira, M. S. Mendes, W. S. Martins, P. L. Saldanha, J. W. R. Tabosa, and D. Felinto, *Phys. Rev. A* **90**, 023848 (2014).
- [9] P. Tighineanu, R. S. Daveau, T. B. Lehmann, H. E. Beere, D. A. Ritchie, P. Lodahl, and S. Stobbe, *Phys. Rev. Lett.* **116**, 163604 (2016).
- [10] H. Jeong, A. M. C. Dawes, and D. J. Gauthier, *Phys. Rev. Lett.* **96**, 143901 (2006).
- [11] J. F. Chen, S. Wang, D. Wei, M. M. T. Loy, G. K. L. Wong, and S. Du, *Phys. Rev. A* **81**, 033844 (2010).
- [12] M. Chalony, R. Pierrat, D. Delande, and D. Wilkowski, *Phys. Rev. A* **84**, 011401(R) (2011).
- [13] C. C. Kwong, T. Yang, M. S. Pramod, K. Pandey, D. Delande, R. Pierrat, and D. Wilkowski, *Phys. Rev. Lett.* **113**, 223601 (2014).
- [14] C. C. Kwong, T. Yang, D. Delande, R. Pierrat, and D. Wilkowski, *Phys. Rev. Lett.* **115**, 223601 (2015).
- [15] S. L. Bromley, B. Zhu, M. Bishof, X. Zhang, T. Bothwell, J. Schachenmayer, T. L. Nicholson, R. Kaiser, S. F. Yelin, M. D. Lukin, A. M. Rey, and J. Ye, *Nat. Commun.* **7**, 11039 (2016).
- [16] M. O. Scully, *Phys. Rev. Lett.* **102**, 143601 (2009).
- [17] S. E. Skipetrov, I. M. Sokolov, and M. D. Havey, *Phys. Rev. A* **94**, 013825 (2016).
- [18] S. Prasad and R. J. Glauber, *Phys. Rev. A* **82**, 063805 (2010).
- [19] I. M. Sokolov, D. V. Kupriyanov, and M. D. Havey, *J. Exp. Theor. Phys.* **112**, 246 (2011).
- [20] I. M. Sokolov, A. S. Kuraptsev, D. V. Kupriyanov, M. D. Havey, and S. Balik, *J. Mod. Opt.* **60**, 50 (2013).
- [21] Y. A. Fofanov, A. S. Kuraptsev, I. M. Sokolov, and M. D. Havey, *Phys. Rev. A* **84**, 053811 (2011).
- [22] Y. A. Fofanov, A. S. Kuraptsev, I. M. Sokolov, and M. D. Havey, *Phys. Rev. A* **87**, 063839 (2013).
- [23] A. S. Kuraptsev and I. M. Sokolov, *Phys. Rev. A* **91**, 053822 (2015).
- [24] S. E. Skipetrov and I. M. Sokolov, *Phys. Rev. Lett.* **114**, 053902 (2015).
- [25] S. Balik, A. L. Win, M. D. Havey, I. M. Sokolov, and D. V. Kupriyanov, *Phys. Rev. A* **87**, 053817 (2013).
- [26] P. W. Milonni and P. L. Knight, *Phys. Rev. A* **10**, 1096 (1974).
- [27] M. J. Stephen, *J. Chem. Phys.* **40**, 669 (1964).
- [28] D. A. Hutchinson and H. F. Hameka, *J. Chem. Phys.* **41**, 2006 (1964).
- [29] R. H. Lehmburg, *Phys. Rev. A* **2**, 883 (1970).
- [30] O. Morice, Y. Castin, and J. Dalibard, *Phys. Rev. A* **51**, 3896 (1995).
- [31] J. Ruostekoski and J. Javanainen, *Phys. Rev. A* **56**, 2056 (1997).
- [32] M. Rusek, A. Orłowski, and J. Mostowski, *Phys. Rev. E* **53**, 4122 (1996).
- [33] H. Fu and P. R. Berman, *Phys. Rev. A* **72**, 022104 (2005).
- [34] I. E. Mazets and G. Kurizki, *J. Phys. B: At. Mol. Opt. Phys.* **40**, F105 (2007).
- [35] A. A. Svidzinsky and J.-T. Chang, *Phys. Rev. A* **77**, 043833 (2008).
- [36] P. W. Courteille, S. Bux, E. Lucioni, K. Lauber, T. Bienaimé, R. Kaiser, and N. Piovella, *Eur. Phys. J. D.* **58**, 69 (2010).
- [37] R. Friedberg and J. T. Manassah, *Phys. Lett. A* **374**, 1648 (2010).
- [38] A. S. Kuraptsev and I. M. Sokolov, *Phys. Rev. A* **90**, 012511 (2014).
- [39] S. D. Jenkins, J. Ruostekoski, J. Javanainen, R. Bourgain, S. Jennewein, Y. R. P. Sortais, and A. Browaeys, *Phys. Rev. Lett.* **116**, 183601 (2016).
- [40] S. D. Jenkins, J. Ruostekoski, J. Javanainen, S. Jennewein, R. Bourgain, J. Pellegrino, Y. R. P. Sortais, and A. Browaeys, *Phys. Rev. A* **94**, 023842 (2016).
- [41] I. M. Sokolov, D. V. Kupriyanov, R. G. Olave, and M. D. Havey, *J. Mod. Opt.* **57**, 1833 (2010).
- [42] S. E. Skipetrov and I. M. Sokolov, *Phys. Rev. Lett.* **112**, 023905 (2014).
- [43] L. Bellando, A. Gero, E. Akkermans, and R. Kaiser, *Phys. Rev. A* **90**, 063822 (2014).
- [44] D. V. Kupriyanov, I. M. Sokolov, C. I. Sukenik, and M. D. Havey, *Laser Phys. Lett.* **3**, 223 (2006).
- [45] G. Labeyrie, *Mod. Phys. Lett. B* **22**, 73 (2008).
- [46] R. Friedberg and J. T. Manassah, *Laser Phys. Lett.* **4**, 900 (2007).
- [47] T. Bienaimé, M. Petruzzo, D. Bigerni, N. Piovella, and R. Kaiser, *J. Mod. Opt.* **58**, 1942 (2011).
- [48] D. V. Kupriyanov, I. M. Sokolov, P. Kulatunga, C. I. Sukenik, and M. D. Havey, *Phys. Rev. A* **67**, 013814 (2003).
- [49] G. Labeyrie, D. Delande, C. A. Müller, C. Miniatura, and R. Kaiser, *Phys. Rev. A* **67**, 033814 (2003).
- [50] V. M. Datsyuk, and I. M. Sokolov, *J. Exp. Theor. Phys.* **102**, 724 (2006).
- [51] J. Chabé, M.-T. Rouabah, L. Bellando, T. Bienaimé, N. Piovella, R. Bachelard, and R. Kaiser, *Phys. Rev. A* **89**, 043833 (2014).
- [52] S. Roof, K. Kemp, M. Havey, I. M. Sokolov, and D. V. Kupriyanov, *Opt. Lett.* **40**, 1137 (2015).
- [53] R. T. Sutherland and F. Robicheaux, *Phys. Rev. A* **93**, 023407 (2016).
- [54] V. M. Datsyuk, I. M. Sokolov, D. V. Kupriyanov, and M. D. Havey, *Phys. Rev. A* **74**, 043812 (2006).
- [55] V. M. Datsyuk, I. M. Sokolov, D. V. Kupriyanov, and M. D. Havey, *Phys. Rev. A* **77**, 033823 (2008).